

Strain relaxation in AlN/GaN bilayer films grown on γ -LiAlO₂(100) for nanoelectromechanical systems

Y. Takagaki,^{a)} Y. J. Sun, O. Brandt, and K. H. Ploog

Paul-Drude-Institut für Festkörperelektronik, Hausvogteiplatz 5-7, 10117 Berlin, Germany

(Received 18 December 2003; accepted 23 March 2004; published online 21 May 2004)

We fabricate submicrometer-wide cantilevers and beams from M-plane AlN/GaN bilayer films grown on γ -LiAlO₂(100) substrates. The chemically reactive substrate is ideal for fabrication of nanoelectromechanical systems using the light, stiff, and piezoelectrically active AlN. The absence of polarization fields in M-plane quantum wells allows us to incorporate optical functionalities in the (Al,Ga)N-based nanoelectromechanical systems. Self-rolling of the cantilevers indicates that the bilayer films are strained at the AlN–GaN interface along the *a* axis, whereas the strain is roughly completely relaxed along the *c* axis. We examine the partial relaxation of the strain along the *a* axis when the layer thickness is varied. © 2004 American Institute of Physics.

[DOI: 10.1063/1.1751224]

Aluminum nitride is a prospective material for nanoelectromechanical systems (NEMS) because of the stiffness (Young's modulus $E = 3.5 \times 10^{11}$ N/m²) and the small mass density ($\rho = 3.23 \times 10^3$ kg/m³). These characteristics have been exploited for successful operations of interdigital transducers to generate surface acoustic waves (SAWs) at frequencies beyond 10 GHz.^{1–3} The material is also unique as the electromechanical coupling coefficient can be as large as 6.5%.⁴ This can be advantageous over typical materials for NEMS, such as Si and Ge, which are not piezoelectric, and GaAs and InAs, in which the electromechanical coupling is weak.

High quality AlN can be grown epitaxially by metalorganic chemical vapor deposition (MOCVD) and molecular-beam epitaxy (MBE). However, the conventional substrates used in epitaxial growth, Al₂O₃ and SiC, are not suitable for selective etching to float the AlN layers up from the substrates. To overcome this problem, Cleland, Pophristic, and Ferguson⁵ used AlN layers grown on Si by MOCVD. The Si substrates can be removed without difficulty using the well-established microfabrication technologies.

In the present work, we report on the fabrication of AlN-based NEMS using a different material system, i.e., AlN/GaN bilayer films grown on γ -LiAlO₂ substrates. The high chemical reactivity of γ -LiAlO₂ provides an almost ideal selectivity for etching to fabricate free-standing plates of AlN/GaN. We investigate the effects of the strain between the AlN and GaN layers, originating from the lattice and thermal-expansion mismatches, on the mechanical properties of the nanoelectromechanical structures.

The growth of AlN and GaN films was carried out by plasma-assisted MBE.⁶ The substrates we used were (100)-oriented γ -LiAlO₂ wafers, which is a tetragonal crystal having the lattice constants of $a = b = 0.51687$ nm and $c = 0.62679$ nm. Under optimized growth conditions, hexagonal AlN and GaN grows with its (1 $\bar{1}$ 00) planes normal to the

growth direction. The [0001] and [11 $\bar{2}$ 0] directions of the epitaxial layers are aligned parallel to the [010] and [001] directions of γ -LiAlO₂, respectively. The growth temperature was 740 °C for both GaN and AlN. The growth rate was 0.27 μ m/h for GaN and 0.22 μ m/h for AlN. The crystal directions of γ -LiAlO₂ were identified using Raman scattering.⁷

The M-plane growth surface provides us distinct material properties in comparison to the C plane of AlN and GaN films grown on Al₂O₃(0001), SiC(0001), and Si(111). In quantum wells consisting of (Ga,Al,In)N layers having the C plane normal to the growth direction, electron-hole recombination is significantly reduced when the well width exceeds about 6 nm due to large built-in electrostatic fields. In contrast, M-plane quantum wells are free from the fields.⁸ Spontaneous polarization is absent because of the nonpolar orientation. In addition, the strain induced by the lattice mismatch does not result in piezoelectric polarization as a consequence of the vanishing strain tensor components ϵ_{31} and ϵ_{32} . The absence of the electrostatic fields is crucial if optical functionalities of GaN and AlN are to be incorporated in NEMS.

When AlN was grown directly on a γ -LiAlO₂ substrate using the growth conditions which have been optimized for GaN, the C plane was aligned normal to the growth direction. Thus, at the moment, we grow an M-plane GaN template prior to the AlN growth. In this manner, the AlN layer is also M-plane oriented. A disadvantage of using the γ -LiAlO₂ substrate is thus the large lattice mismatches between AlN and GaN. We summarize the expected strains along the *a* and *c* axes in Table I. The GaN lattice constants

TABLE I. Mismatches $\epsilon = \Delta a/a$ and $\Delta c/c$ of the lattice constants in the [11 $\bar{2}$ 0] and [0001] directions of AlN and GaN, respectively. A positive (negative) value indicates that the layer on the left-hand side is tensile (compressive) strained with respect to the material on the right-hand side.

	$\Delta a/a$	$\Delta c/c$
AlN/GaN	2.37%	3.91%
GaN/ γ -LiAlO ₂	-1.67%	-0.3%
AlN/ γ -LiAlO ₂	0.70%	3.61%

^{a)}Author to whom correspondence should be addressed; electronic mail: takagaki@pdi-berlin.de

TABLE II. Parameters of three AlN/GaN/ γ -LiAlO₂ heterostructures 1–3. The thicknesses of the AlN and GaN layers are h_{AlN} and h_{GaN} , respectively. The radii of the loops due to the self-rolling are r_a and r_c in the [11 $\bar{2}$ 0] and [0001] directions of the bilayer films, respectively. The strains estimated from r_a and r_c are shown in the columns $\Delta a/a$ and $\Delta c/c$, respectively.

	h_{AlN} (nm)	h_{GaN} (nm)	r_a (μm)	$\Delta a/a$ (%)	r_c (μm)	$\Delta c/c$ (%)
1	45	120	11	1.0	...	$\ll 1$
2	70	110	14	0.7	39	0.3
3	350	515	276	0.2

are slightly larger than required for a perfect fit to the unit mesh of γ -LiAlO₂, resulting in compressive strains, whereas the opposite occurs with AlN on γ -LiAlO₂ and it is tensile strained. To utilize the bilayer system, it is, therefore, necessary to understand the residual strains at the AlN–GaN interfaces and their influences on the mechanical properties of NEMS. We emphasize that thermal stress is critical in III-nitrides because of their rather high growth temperature. In our investigations, we employ three heterostructures. We list the thicknesses of the AlN and GaN layers in Table II. The film thicknesses were measured using cross-sectional scanning electron microscope (SEM) images.

The patterns of submicrometer-wide cantilevers and beams were delineated using electron-beam lithography and the lift-off technique. This process leaves thin-film structures composed of Au–NiCr multilayers on the AlN surface, which are to be used as an etch mask for reactive ion etching (RIE). The AlN/GaN epilayers were removed by RIE using a mixture of Cl₂ and Ar gases. The flow rates were 2 and 10 sccm for Cl₂ and Ar, respectively. We used a rf power of 50 W. The plasma voltage was 160 V. The etch rate for the composite nitride layers was about 10 nm/min. The γ -LiAlO₂ substrate was then etched using a HCl solution. Narrow strips of the AlN/GaN layers were attached to large pads, which served as supporting pillars, either at one end or both ends. Cantilevers and beams were hence detached from the substrates. The substantial chemical reactivity of γ -LiAlO₂ and nonreactivity of AlN and GaN give rise to almost perfect selectivity for etching.

In Fig. 1, we show SEM images of the beams, (a) and (b), and the cantilevers, (c) and (d). Their widths are about

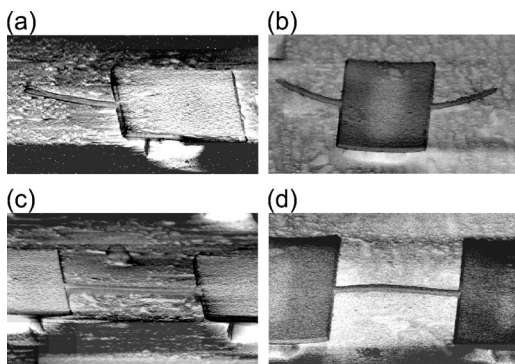


FIG. 1. Scanning electron micrograph of 200-nm-wide cantilevers, (a) and (b), and beams, (c) and (d). The cantilevers are 4.0 μm long and the beams are 6.0 μm long. The narrow strips of the AlN/GaN bilayer system extend in the [0001] direction in (a) and (c) and in the [11 $\bar{2}$ 0] direction in (b) and (d). The thicknesses of the AlN and GaN layers are, respectively, 45 and 120 nm, i.e., heterostructure 1.

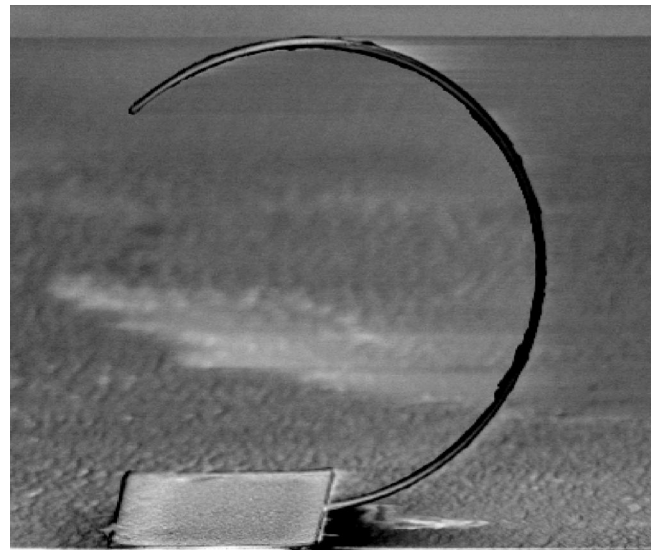


FIG. 2. Scanning electron micrograph of a loop composed of the AlN/GaN bilayer system created by the strain-induced self-rolling. The strip stretches in the AlN[11 $\bar{2}$ 0] direction. The width of the strip is 1 μm . The radius of the loop is 11 μm . The thicknesses of the AlN and GaN layers are, respectively, 45 and 120 nm, i.e., heterostructure 1.

200 nm. The lengths are 6.0 μm for the beams and 4.0 μm for the cantilevers. The wet etching for the γ -LiAlO₂ substrates was carried out 0.5–1 μm deep. The suspension pads were thus under etched by the same extent. Notice that these nanoelectromechanical structures are bowed upwards. The degree of the rolling differs between the structures stretched along the a axis, (a) and (c), and the c axis, (b) and (d). The bowing originates from the self-rolling of highly strained heterostructures.^{9–13} The cantilevers are concave shaped as the lattice constant of AlN is less than that of GaN. This shape is, however, modified in Fig. 1(d) as the beam is clamped at the two ends. In the latter case, the shape is determined by two factors: the lattice mismatch at the AlN/GaN interface and the stress that the bilayer film experiences from the γ -LiAlO₂ substrate. The bilayer film is compressively stressed by the substrate, and so the beam is convex shaped at the middle. By increasing the length of the cantilevers, a loop can be eventually formed, as shown in Fig. 2. The self-rolling has been proposed to be a method to prepare nanotubes of any size at almost arbitrary locations.¹⁴ The present material system can be used for such purposes as well.

Within the continuum elasticity theory, the radius r of the loop is given by¹⁵

$$r = \frac{h_1^4 + 4\chi h_1^3 h_2 + 6\chi h_1^2 h_2^2 + 4\chi h_1 h_2^3 + \chi^2 h_2^4}{6\epsilon\chi(1+\nu)h_1 h_2 (h_1 + h_2)}, \quad (1)$$

where ϵ is the lattice mismatch and h_1 and h_2 are the thicknesses of the bilayer films. Here, $\chi = E_2/E_1$, while Poisson's ratio ν is assumed to be identical for the two layers. If we approximate $\chi = 1$,^{9–12} the radius for a fixed total layer thickness ($h_1 + h_2 = \text{const}$) is minimal, $r_{\text{min}} = 8h_1/[6\epsilon(1+\nu)]$, when $h_1 = h_2$. Notice that the radius is, in principle, proportional to the film thickness. The anisotropy of Young's modulus E is described for hexagonal crystals as

$$E^{-1} = s_{11} \sin^4 \theta + s_{33} \cos^4 \theta + (s_{44} + 2s_{13}) \sin^2 \theta \cos^2 \theta, \quad (2)$$

where s_{ij} are the elastic compliance constants and θ is the angle of the stress direction relative to the c axis. We hence obtain $E_c = s_{33}^{-1} = C/(c_{11} + c_{12})$ along the c axis and $E_a = s_{11}^{-1} = 2/[c_{33}/C + (c_{11} - c_{12})^{-1}]$ along the a axis with $C = c_{33}(c_{11} + c_{12}) - 2c_{13}^2$. Here, c_{ij} are the elastic stiffness constants. The constants evaluated by fitting the dispersion of the SAWs in the layered system give $E_c = 3.43$ and 3.54×10^{11} N/m² and $E_a = 3.01$ and 3.50×10^{11} N/m² for GaN and AlN, respectively.⁷

In Fig. 2, the cantilever extends along the a axis. The experimental observation of $r = 11 \mu\text{m}$ gives $\epsilon = \Delta a/a = 0.99\%$ assuming $\nu = 0.22$. The value is considerably lower than the expected mismatch of 2.37%. Moreover, although the lattice mismatch is larger along the c axis than along the a axis, the rolling radius along the c axis was much larger than that along the a axis in all of the three heterostructures. These observations suggest plastic relaxations of the strain at the AlN–GaN interfaces. We note that the disagreement of the coiling radius between the experimental results and the theoretical predictions might be attributed to the chemical modifications of the surfaces.^{9,10} However, we rule this out because of the chemical stability of the AlN and GaN surfaces. Moreover, the surface effects are insignificant in our devices due to the large layer thicknesses.

In Table II, we summarize the strains evaluated as described above in three heterostructures having different film thicknesses. For heterostructure 1, the long cantilever along the c axis collapsed onto the substrate due to the surface tension of the wet etch solution.¹⁶ This implies that the bowing in the $[0001]$ direction was not large enough to move the cantilever away from the substrate, i.e., it was significantly less than that in the $[11\bar{2}0]$ direction, cf. Fig. 1(a). The strain along the c axis is thus clearly indicated to be less than that along the a axis, although a quantitative evaluation was not possible.

The strain is roughly completely relaxed along the c axis, whereas it is only partly relaxed along the a axis. The lattice mismatch along the c axis is indicated to be too large to be retained during the epitaxial growth. The same conclusion was also reached by high-resolution transmission electron microscopy (TEM).¹⁷ One can neglect the difference in the thickness of the GaN bottom layer in considering the strain at the AlN–GaN interfaces. The optical transmittance has revealed that the GaN layers on γ -LiAlO₂ are almost

fully strained even when the thickness is as large as 700 nm.¹⁸ The partial strain relaxation along the a axis is thus seen to be enhanced when the AlN top layer becomes thicker.

In conclusion, we have employed the AlN/GaN bilayer films grown on γ -LiAlO₂(100) substrates for fabrication of NEMS. The advantages of this material system are (1) the nearly ideal etch selectivity between the epilayers and the substrates and (2) the absence of polarizations in the M-plane AlN and GaN layers. By analyzing the self-rolling of cantilevers, we have shown that the strain at the AlN–GaN interfaces is almost completely relaxed along the c axis. The strain along the a axis is relaxed moderately with an increase in the top layer thickness.

The authors would like to thank E. Wiebicke and A. Schönrock for their assistances in the sample processing and M. Ramsteiner for the Raman scattering measurements. This work was supported in part by the Deutsche Forschungsgemeinschaft and by the NEDO collaboration program.

¹ Y. Takagaki, P. V. Santos, E. Wiebicke, O. Brandt, H.-P. Schönherr, and K. H. Ploog, Appl. Phys. Lett. **81**, 2538 (2002).

² Y. Takagaki, O. Brandt, and K. H. Ploog, Jpn. J. Appl. Phys., Part 1 **42**, 1594 (2003).

³ Y. Takagaki, T. Hesjedal, O. Brandt, and K. H. Ploog, Semicond. Sci. Technol. **19**, 256 (2004).

⁴ O. Ambacher, J. Phys. D **31**, 2653 (1998).

⁵ A. N. Cleland, M. Pophristic, and I. Ferguson, Appl. Phys. Lett. **79**, 2070 (2001).

⁶ Y. J. Sun, O. Brandt, and K. H. Ploog, J. Vac. Sci. Technol. B **21**, 1350 (2003).

⁷ Y. Takagaki, C. Hucho, E. Wiebicke, Y. J. Sun, O. Brandt, M. Ramsteiner, and K. H. Ploog, Phys. Rev. B **69**, 115317 (2004).

⁸ P. Waltereit, O. Brandt, A. Trampert, H. T. Grahn, J. Menniger, M. Ramsteiner, M. Reiche, and K. H. Ploog, Nature (London) **406**, 865 (2000).

⁹ V. Y. Prinz, V. A. Seleznev, A. K. Gutakovskiy, A. V. Chehovskiy, V. V. Preobrazhenskii, M. A. Putyato, and T. A. Gavrilova, Physica E (Amsterdam) **6**, 828 (2000).

¹⁰ S. V. Golod, V. Y. Prinz, V. I. Mashanov, and A. K. Gutakovskiy, Semicond. Sci. Technol. **16**, 181 (2001).

¹¹ A. B. Vorob'ev and V. Y. Prinz, Semicond. Sci. Technol. **17**, 614 (2002).

¹² A. Vorob'ev, V. Prinz, V. Preobrazhenskii, and B. Semyagin, Jpn. J. Appl. Phys., Part 2 **42**, L7 (2003).

¹³ O. G. Schmidt and N. Y. Jin-Phillipp, Appl. Phys. Lett. **78**, 3310 (2001).

¹⁴ O. G. Schmidt and K. Eberl, Nature (London) **410**, 168 (2001).

¹⁵ M. Grundmann, Appl. Phys. Lett. **83**, 2444 (2003).

¹⁶ H. Namatsu, K. Yamazaki, and K. Kurihara, J. Vac. Sci. Technol. B **18**, 780 (2000).

¹⁷ TEM measurements have shown that the strain relaxation at the AlN/GaN interfaces occurs via the formation of partial dislocations, which are associated with basal plane stacking faults. See, T. Y. Liu, A. Trampert, Y. J. Sun, O. Brandt, and K. H. Ploog, Philos. Mag. Lett. (in press) and T. Y. Liu, Ph.D. dissertation, Humboldt Universität, Berlin, 2004.

¹⁸ P. Misra, Y. J. Sun, O. Brandt, and H. T. Grahn (unpublished).